

Featuring work from Yanbo Xie and Jan Eijkel at the BIOS/Lab on a Chip group at the MESA+ Institute for Nanotechnology, University of Twente.

Title: Pressure-driven ballistic Kelvin's water dropper for energy harvesting

A self-excited ballistic energy conversion device is presented, inspired by Kelvin's water dropper. Kelvin's design was improved on two crucial points: using inertia instead of gravity allows much higher energy densities and introducing non-linear gate feedback gives stable and efficient energy conversion.

As featured in:



See Jan C. T. Eijkel *et al.*, *Lab Chip*, 2014, 14, 4171.



[www.rsc.org/loc](http://www.rsc.org/loc)

Registered charity number: 207890



## Pressure-driven ballistic Kelvin's water dropper for energy harvesting†

 Cite this: *Lab Chip*, 2014, 14, 4171

 Received 24th June 2014,  
Accepted 28th July 2014

 Yanbo Xie,‡ Hans L. de Boer, Ad J. Sprenkels, Albert van den Berg  
and Jan C. T. Eijkel\*

DOI: 10.1039/c4lc00740a

[www.rsc.org/loc](http://www.rsc.org/loc)

In this paper, we introduce a microfluidic-based self-excited energy conversion system inspired by Kelvin's water dropper but driven by inertia instead of gravity. Two micro water jets are produced by forcing water through two micropores by overpressure. The jets break up into microdroplets which are inductively charged by electrostatic gates. The droplets land on metal targets which are gradually charged up to high voltages. Targets and electrostatic gates are cross-connected in a way similar to Kelvin's water dropper. Application of pressure as driving force instead of gravity as in Kelvin's dropper allows for much higher energy densities. To prevent overcharging of the droplets by the inductive mechanism and consequent droplet loss by repulsion from the target as in Kelvin's water dropper, a voltage divider using inversely connected diodes was introduced in our system to control the charge induction providing self-limiting positive feedback by the diode characteristics. A maximal 18% energy conversion efficiency was obtained with the diode-gated system.

### Introduction

As one of the renewable energy conversion methods, microfluidic energy conversion is relatively unknown to the public. Recently, we have demonstrated a new form of microfluidic energy conversion termed as "ballistic", which is both an efficient and a powerful method to generate electric power. We showed that with a single-jet system a maximal conversion efficiency of 48% could be obtained.<sup>1</sup> In this conversion method, water is accelerated by pumping it through a micropore, where it forms a microjet breaking up into fast-moving ( $>10 \text{ m s}^{-1}$ ) charged droplets. Droplet kinetic energy is subsequently converted to electrical energy when the charged droplets decelerate in the electrical field that forms between a membrane and a metal target. Like traditional electrostatic

gate control in micro/nanofluidics,<sup>2,3</sup> in our original device we also employed an electrostatic gate to charge the droplets and obtained a stable and adjustable current generation that is independent of the membrane zeta potential. With a well-controlled applied voltage and proper design of the gate, theoretically the droplet charge density can be increased up to the Rayleigh limit, so that the target potential required for high efficiency can be decreased to the order of daily-use range.<sup>1</sup> However, for an electrical energy conversion device, an external voltage source is cumbersome to implement. Instead, a self-excited energy conversion system will be much more convenient for applications, as it is in many other self-excited energy devices that have been studied.<sup>4–8</sup> Here we report on such a self-excited device.

Lord Kelvin invented an electrostatic high-voltage generator by water dripping in 1867, generally named the 'Kelvin water dropper'.<sup>9</sup> Two metal buckets with an opening at the bottom drip water. The falling water drops pass through hollow metal rings and are collected by two other metal buckets. The hollow metal rings through which the droplets pass are cross-connected with both bottom buckets (a setup as in Fig. 2a). As a result, any tiny charge on the water drops (e.g. a positive charge) that left the top left bucket will charge the bottom left bucket and hence the right side ring. The metal ring on the right side will then attract more negative charges to the water drops on the right side, so that more net negative charges will be collected by the bottom right bucket and the negative voltage increases on the left ring. Hence, a positive feedback exists and the two downstream buckets will continue this charging process until voltage breakdown occurs between the two bottom buckets, or drops are repelled and fall outside of the buckets. The Kelvin water dropper is thus a self-excited positive feedback system that charges water droplets and delivers charged droplets at high electrical potential driven by gravity.<sup>10</sup> A first step towards a practical useful voltage generator based on Kelvin's water dropper was shown recently, when Marín *et al.* demonstrated a microfluidic version of Kelvin's water dropper using water-in-oil droplets.<sup>11</sup> Also a self-powered ionization device can be produced

BIOS-Lab on a Chip Group, MESA+ Institute for Nanotechnology, University of Twente, The Netherlands. E-mail: j.c.t.eijkel@utwente.nl

† Electronic supplementary information (ESI) available. See DOI: 10.1039/c4lc00740a

‡ Present address: School of Science, Department of Applied Physics, Northwestern Polytechnical University, PR China.

based on Kelvin's water dropper where ionization occurs at very low potentials by providing very low internal energy to the ions.<sup>12</sup> However, the Kelvin water dropper itself has not been further improved as an energy harvesting device since the droplets are easily overcharged, inducing much deflection (loss) of droplets on energy collection. Besides, the generated voltage is far too high for practical applications, and the harvested currents are very small with regard to the amount of water consumed.

Previously, we demonstrated the single microjet ballistic system discussed above.<sup>1</sup> In the present paper, we apply an electrostatic charge self-induction mechanism inspired by Kelvin's water dropper to this inertia-driven (ballistic) energy conversion system and show that the disadvantages of Kelvin's water dropper can be overcome. The droplet charge will be derived from the same inductive charging mechanism as in Kelvin's droplet generator, employing two separate systems and cross-connecting targets and induction rings. As already mentioned above, one of the disadvantages of Kelvin's water dropper is that it uses a positive feedback system that is inherently unstable since the droplet charge keeps increasing until the droplets are deflected from the target because the work (required for droplets landing) done by electrical force overcomes the gravitational force ( $mgh < qU_{\text{target}}$ ), where  $m$ ,  $g$  and  $h$  are the droplet mass, the acceleration due to gravity and the bucket height, respectively,  $q$  is the charge quantity in the droplets, and  $U_{\text{target}}$  is the target voltage. In our ballistic system, overcharging of droplets will also result in droplet repulsion from the target, when the droplet kinetic energy  $1/2mv^2$  is smaller than the electrical energy  $qU_{\text{target}}$  which the droplets would deliver when they reach the target ( $1/2mv^2 < qU_{\text{target}}$ ). Here  $m$ ,  $v$ , and  $q$  are the mass, velocity and charge quantity in droplets, respectively, and  $U_{\text{target}}$  is the target voltage. The deflection of these overcharged droplets causes a lower efficiency.<sup>1</sup> To overcome the disadvantages of Kelvin's positive feedback mechanism, we therefore introduce voltage dividers (including an ohmic and a non-ohmic divider by reversely connecting diodes) in the system to properly control the

induction voltages, thus enabling a stable current generation and energy conversion as a self-gated system.

## Ballistic Kelvin's water dropper – principle and setup

As we described previously, the energy conversion in a ballistic system can be influenced by using an induction ring to control the charge density of the droplets and hence the current carried by the droplets. A negative applied voltage on the gate (induction) ring thereby induces a positive current  $I_1$  in the upstream reservoir. To investigate the possibility of inducing both a positive and a negative current by gate induction, as needed for a self-excited operation, we performed a preliminary experiment (setup shown in the inset of Fig. 1a). As shown, the current can be tuned from positive (75 nA) to negative (−83 nA) by adjusting the applied gate voltage from −600 V to 650 V with a power source (Keithley 2410). The electrostatic induction of charges in the liquid jet is a capacitive process, and the resulting charge quantity in the droplets can be calculated as  $q = C_{\text{ind}} \times U_{\text{target}}$ , where  $q$  and  $C_{\text{ind}}$  are the charge quantity in the droplets and the capacitance of the induction gate, respectively, which is a function of the induction ring dimension and its distance from the jet.<sup>13</sup> The induction charge (current) thus is expected to increase linearly with the applied voltage as indeed observed in Fig. 1a. Hence, we can conclude that adjusting the voltage on the gate ring enables not only quantities but also polarities of the droplet charge density. This provides a possibility to use the design of the Kelvin water dropper to build a self-excited ballistic energy conversion device.

Fig. 1b shows a schematic picture of our ballistic Kelvin's water dropper energy conversion device. Two silicon nitride membranes with a single cylindrical pore with a diameter of 30  $\mu\text{m}$  were mounted on pressurized PMMA reservoirs with rubber O-rings. The reservoirs contained degassed ultrapure 10 mM KCl solution. A layer of 150 nm thick Pt was sputtered at the back side of the chip for electrical connection with instruments *via* four metal pins. The mechanical input power

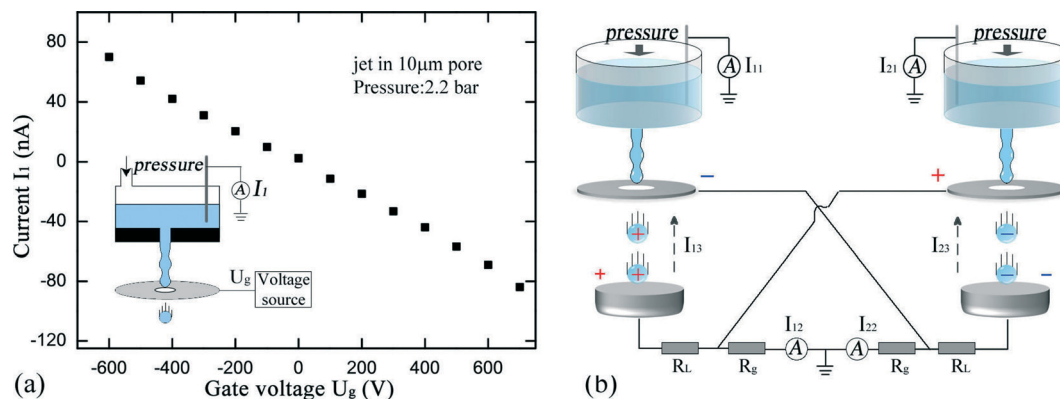


Fig. 1 a. The principle of controlling the upstream current by gate induction. The polarity of current  $I_1$  can be controlled by applying a proper gate voltage. Solution, 0.1 M KCl; pore diameter, 10  $\mu\text{m}$ ; applied pressure, 2.2 bar. b. Our self-excited ballistic energy system driven by pressure. Resistors form a voltage divider to separate the gate voltage from the target voltage.

can be calculated by measurement of the flow rate (Bronkhorst Cori-flow flow sensor) and pressure (Sensortech CTE 8016 GY7 pressure sensor). Two pieces of aluminum foil with a thickness of 0.2 mm were attached under the chip holders to function as an induction gate. Upstream currents are denoted as  $I_{11}$  and  $I_{21}$ , and the harvested currents are denoted as  $I_{12}$  and  $I_{22}$ . The currents, including the current generated by deflection of droplets from the target to the gate ring ( $I_{13}$  and  $I_{23}$ ), can be measured by either a pico-ammeter (Keithley) or a multi-meter in voltage mode, showing the voltage difference over its integrated 10 M $\Omega$  resistor induced by the current flow. Two stainless steel cups functioned as targets and were placed beneath the chip holders to collect charged droplets. The load resistance connected between these targets and ground was divided into two sections: resistors for electrical power generation and resistors for induction of the other jet, denoted as  $R_L$  and  $R_g$ , respectively. Resistors were immersed in an oil bath (Shell Diala S2-ZU-I) to prevent corona discharge and a layer of Delrin (polyoxymethylene) was mounted on the edge of the cup for the same reason, at the location where the electrical field was expected to be the strongest.

## Experimental results

### Kelvin's connection

In view of the successful generation of high voltage by Kelvin's water dropper, we first directly apply Kelvin's water dropper electrical connection in our ballistic energy

conversion system (see Fig. 2a). To understand how the system functions, we can extract the electrical elements from the setup and make a simple circuit drawing as shown in Fig. 2b. Electrical currents  $I_{11}$  and  $I_{21}$  carried by the two jets were successfully generated with magnitudes of up to 60 nA. The upstream currents from the two jets had opposite polarities, showing successful operation in current induction mode. However, almost no charged droplets were collected by the targets, as they were deflected to the gate as could be observed by the naked eye and were expressed in low values of the downstream collected currents  $I_{12}$  and  $I_{22}$ . These deflected droplets can be considered as a negative feedback to the gate voltage that keeps the droplet charge density at a proper level for stable operation. However, the deflection of droplets represents an energy loss source as it decreases the useful current through load resistance  $R_L$ . In addition, the deflected droplets contacting the gate electrodes decrease the current flow through  $R_g$ , thus doubling the electrical energy losses on  $R_g$  since the total output energy can be calculated as  $P_{\text{out}} = [(I_{12} + I_{23})^2 + (I_{22} + I_{13})^2] \times R_L + (I_{12}^2 + I_{22}^2) \times R_g$ . As expected, the weakness of this electrical setup is caused by the fact that the target is directly connected to the gate as in Kelvin's water dropper, and hence target voltage equals gate voltage. Gate voltages (and hence induced droplet charges) thereby become much higher than the ones needed for efficient operation. Thus, we introduced a voltage divider in the target circuit to independently control target voltage and gate voltage.

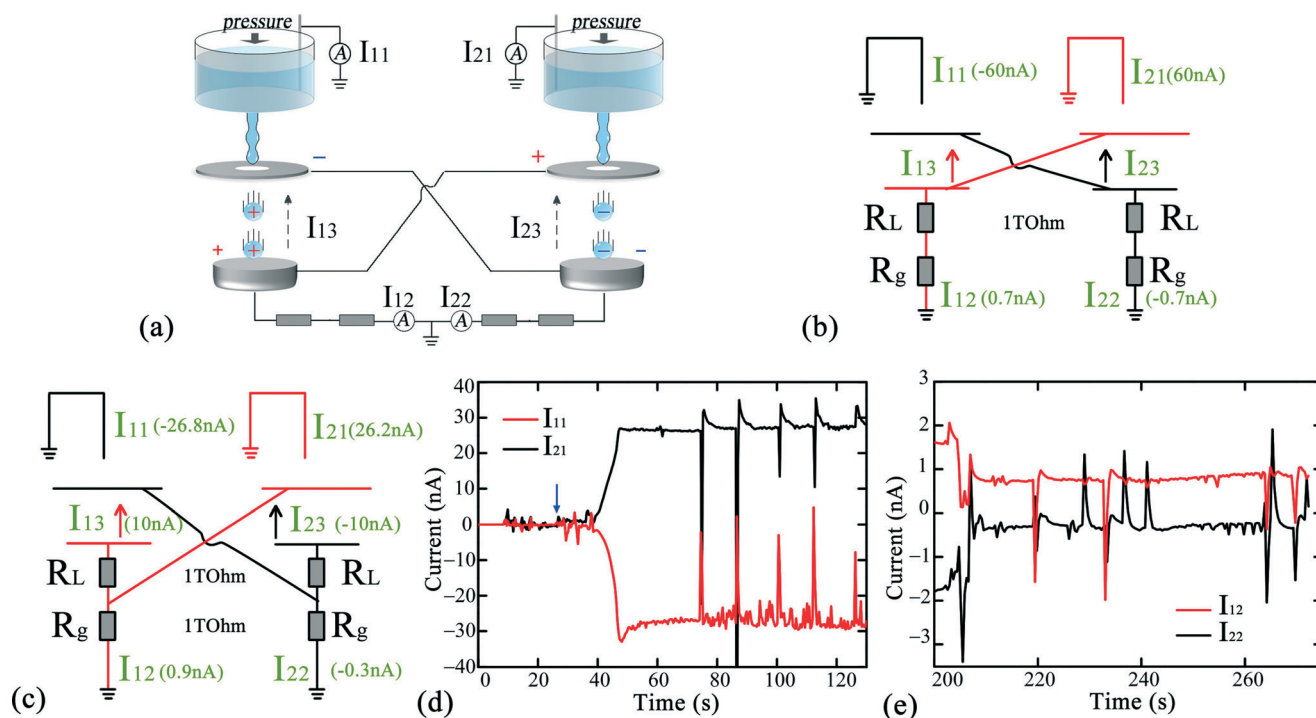


**Fig. 2** Measurements using the self-induction system. a. A schematic picture of the typical connection of Kelvin's water dropper. Induction rings are directly connected to the bottom targets. b. The connection scheme of Kelvin's water dropper. Most droplets are highly charged and are deflected to the gate ring. c. The connection scheme with voltage divider. d. Using the voltage divider, the upstream currents  $I_{11}$  and  $I_{21}$  increase as a function of time. The blue arrow indicates when the induction gate was connected. e. Using the voltage divider, both downstream currents  $I_{12}$  and  $I_{22}$  are only a fraction of the upstream currents after some time of operation.

## Resistor voltage divider connection

Two downstream circuits were investigated to perform self-induction. First, two 1 T $\Omega$  resistors were series connected for power generation and gate induction (Fig. 2c). In Fig. 2d, we can see clearly that the upstream currents  $I_{11}$  and  $I_{21}$  increase rapidly after the upper electrodes were connected to the ammeter (the event is marked by a blue arrow). Deflected droplets accumulated at the bottom of the gate, dripping to the target and causing the observed periodic transients in current level. Operation was still not optimal, since from Fig. 2e it can be seen that the downstream currents  $I_{12}$  and  $I_{22}$ , which are the currents through  $R_g$ , were still much smaller than the upstream currents, again due to partial deflection of the charged droplets.

As one of the most important performance characteristics of an energy conversion device, we calculate the efficiency which is defined as the ratio of electrical output power ( $P_{out}$ ) to fluid mechanical input power ( $P_{in}$ ),  $eff = P_{out}/P_{in}$ . We determine the electrical output power  $P_{out}$  by measuring the current ( $I_{i2}$ ) flow through  $R_g$  and then deriving the current flowing through  $R_L$  by applying Kirchhoff's current law at the junction of  $R_g$  and  $R_L$ , stating that the current through  $R_L$  equals the sum of the currents through the gate and  $R_g$ . The output power of the two jets thus calculated is 226  $\mu$ W. From measurements of the flow rate (13.1  $\mu$ L s $^{-1}$ ) and applied pressure (1.40 bar), the efficiency of the resistive current divider system is calculated as 12.3%.

This efficiency is much lower than what we previously showed in a single jet with gate control *via* an external voltage source (48%).<sup>3</sup> A possible explanation for this lower efficiency is that  $R_g$  is still too high for proper charge induction. As shown in Fig. 1a, the induction charge increases linearly with gate voltage. For instance, assuming that no current loss occurs by deflected droplets, 10 nA creates 10 kV on the gate ring, which is too high for current induction in our system according to our previous research (nearly  $-170$  V gate voltage was found to be optimal for  $R_L = 1$  T $\Omega$ ).<sup>1</sup> Another reason for the low efficiency is that the highly charged droplets repel each other and form a cone when they move out of the gate, as was indeed observed (Fig. S3 $\dagger$ ). The flat top surfaces of the targets induce a trajectory distance difference for the droplets at the outside and inside of the cone, implying that the distances are no longer optimal for part of the droplets, thus generating lower efficiency. Besides, a cone forms less air wake compared to a straight droplet train so that in general the energy losses against air friction forces increase. Compared with Kelvin's induction mode, when a voltage divider was used the induction currents in the top circuits were close to the optimal value for such a system as shown before.<sup>1</sup> Besides, much higher currents were collected at the load resistance, enabling a higher energy conversion efficiency.

To further optimize the system, we investigated a much lower gate resistance ( $R_g < 10$  G $\Omega$ ) in the same symmetric connection, with the aim of tuning  $R_g/(R_L + R_g)$  to create the optimal fraction of operation gating voltage over target

voltage observed in our previous investigations ( $U_g/U_{target} = 170$  V/20 kV).<sup>1</sup> However, in the experiments only a slight upstream current was induced, remaining constantly small within at least 10 min. To explain this observation, we derived a general induction model which is presented below, where we will show that in general it is impossible to avoid either positive or negative feedback in an ohmic divider system.

## Diode voltage divider

As observed in the above experiments and explained in the induction model section below, an ohmic resistive voltage divider either overcharges or does not charge the droplets. To induce a stable current and consequently obtain a stable energy conversion, we therefore decided to introduce elements with a non-linear resistance behavior for the electrostatic gating in the circuit. We applied reversely connected diodes for this purpose, which exhibits an ohmic behavior at low currents and a constant voltage drop at high currents. The benefits of adding these reversely connected diodes are that the induction voltage can now become a constant independent of target voltages (or downstream current), while the induction mechanism will still work. As a result, the gate voltage can stay in a constant suitable range preventing overcharging of the droplets. The  $I$ - $V$  curve of the reversely connected diode used is shown in Fig. S1 $\dagger$ . An exponential fit to the measured diode data showed that the diodes have a non-ohmic resistance behavior described by  $U_g = 533 \times (1 - \exp(-0.55 \times I_i))$ , where  $I_i$  is the current through the diode in reversed polarity (see Fig. S1b $\dagger$ ).

In the setup, we furthermore added a second forward connected diode in series to prevent random charging of the two microjets (Fig. 3b). When the pressure was increased, the initial current was less than 1 nA and was generated by the microjet due to the sum of the streaming current and initial induction current (Fig. 3a). This value is lower than the streaming current measured in pure water solution (about 3 nA) because the use of a salt solution (10 mM KCl) to facilitate inductive charging decreases the membrane surface zeta potential. The current then rapidly increased when the current flow through the diodes generated an induction voltage. Above 15 nA, the current started to saturate, finally reaching a plateau around 19 nA. Fig. 3a also shows two fitted curves (dashed lines) obtained from a resistor divider model and a diode divider model (see the induction model section), respectively. It can be seen that the noise in the saturated current section is somewhat larger but much smaller than the noise caused by deflected droplets landing on the gate. No periodic transients were observed in the current measurements within an observation period of 5 minutes, indicating that the amount of deflected droplets did not lead to water dripping from the gate. We attribute this noise to transient instability of the jet. One thing that needs to be noted in Fig. 3b is that the induction currents for the two jets are different. This can be explained by slight variations of the

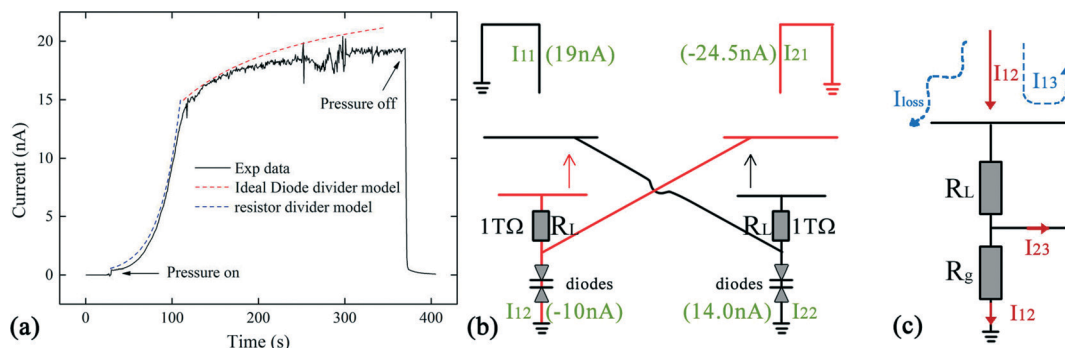


**Fig. 3** a. The rise in current  $I_{11}$  as a function of time when the feedback circuit with diodes is used as shown in b. A clear current saturation is observed and the current disappears immediately when the pressure is turned off. The blue dashed line shows the theoretical prediction using an ohmic resistor ( $R_g/(R_L + R_g) = 0.02$ ) divider by our induction model, where  $R_g$  here is the equivalent resistance of a reversely connected diode. The red dashed line shows the prediction by using a reversely connected diode divider ( $nC_{\text{ind}} = 0.05 \text{ nA V}^{-1}$ ,  $C_L = 12 \text{ pC}$ ). b. Scheme of the electrical circuit and values of the measured currents. The efficiency can be calculated by simultaneous measurement of flow rate and pressure. c. Schematic picture of the current loss and gain in the circuit, taking the left jet as an example.  $R_g$  represents the resistance of diodes. The measured current is a low estimate of current downstream due to partial current leakage from the (right side) gate ring.

gate ring positions, inducing differences of the induction capacitance of the two jets; also, the small differences in saturation voltage of the diodes will result in different induction voltages and hence induction currents.

It can be seen from Fig. 3b that a much higher downstream current than in the case of the resistor gating (Fig. 2) was obtained, which can be explained by the lower amount of deflected droplets. The target voltage can be approximately calculated by the sum of the voltage over the resistor and the diodes (about 500 V when the downstream current is over 4 nA). From the measured flow rate for the two microjets ( $12.3 \mu\text{L s}^{-1}$ ) and the applied pressure (1.40 bar), we then calculate that the total efficiency of the self-excited system is at least 18%. The current flow diagram is shown in Fig. 3c, taking the left side jet as an example. Current generated by the jet has three destinations: landed on target, deflected and lost elsewhere, while the latter two do not contribute to the energy conversion. Besides, the measured downstream current is a low estimate due to partial current flow through the right side gate because of the opposite polarity of the droplets landing on the (right side) gate ring. There is still room to improve the performance of this device, such as by changing the orifice diameter of the gate ring, optimal design of the target and optimizing the choice of the diodes. For example, the droplets partially landed on the Delrin covers ( $I_{\text{loss}}$  in Fig. 3c), leading to a loss of electrical energy. A more optimal design of the complete setup will thus be useful for improving the energy conversion efficiency.

### Induction model

An equivalent circuit to model the induction mechanism in the present device is shown in Fig. 4. Different from Kelvin's generator, both targets are connected to ground by resistors and voltage dividers are used for charge induction. The charge induction behavior can be considered to control the two current sources of the jets similarly to a field

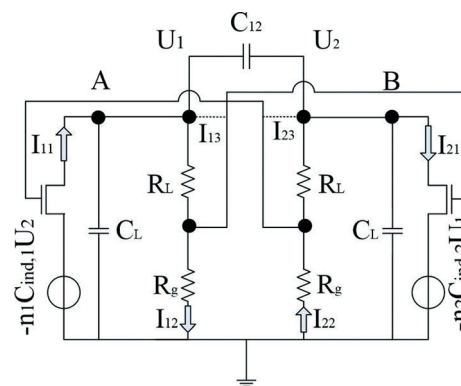


**Fig. 4** An equivalent circuit to model the induction mechanism in the ballistic Kelvin's water dropper. The two current sources represent the two jets 1 and 2 through which a current  $I_{11}$  flows proportional to the gate voltage  $m_j U_j$ , the effective gate capacitance expressed per droplet  $C_{\text{ind},i}$  and the droplet frequency  $n_i$ . For simplicity, we do not consider current loss ( $I_{13}$ ,  $I_{23}$ ) and charge release between two targets ( $C_{12}$  is infinitely small); the current  $I_i$  through the load plus target resistor charges the target capacitance  $C_L$ , and after sufficient time, the target reaches a voltage equal to  $I_i/(R_L + R_g)$ .

effect transistor (FET), with a current described for jet 1 by  $I_{11} = -n_1 C_{\text{ind},1} (m \cdot U_2)$ , where  $n_1$  and  $C_{\text{ind},1}$  are the generation frequency of droplets and the effective induction capacitance of gate 1 for a single droplet, respectively, and  $m$  and  $U_2$  are the fractional voltage division ( $m = R_g/(R_L + R_g)$ ) and the (opposite) target voltage, respectively.  $R_g$  is formed by either a resistor or an inversely connected diode. Here the minus sign indicates the reverse polarity of the induction current and target voltage. Similarly, we can calculate the induction current on the other side as  $I_{21} = n_2 C_{\text{ind},2} (m \cdot U_1)$ .<sup>14</sup> To simplify the model, we do not discuss deflected droplets here, so that jet current equals current through the load.

By Kirchhoff's law, the sum of the currents flowing in and out at nodes A and B is zero. The currents at nodes A and B can be described as follows:

$$-m n C_{\text{ind}} U_2 = U_1 / (R_L + R_g) + C_L \frac{dU_1}{dt} \quad (1)$$

$$-m n C_{\text{ind}} U_1 = U_2 / (R_L + R_g) + C_L \frac{dU_2}{dt} \quad (2)$$

Here we assume that the single droplet current induction capacitances  $C_{\text{ind}}$  for both jets are equal. By solving these equations, we obtain the generated voltage as a function of time.

$$U_1 = A \exp\left(\left(\frac{nmC_{\text{ind}}}{C_L} - \frac{1}{RC_L}\right)t\right) \quad (3)$$

$$U_2 = -A \exp\left(\left(\frac{nmC_{\text{ind}}}{C_L} - \frac{1}{RC_L}\right)t\right) \quad (4)$$

Hereby  $A$  is a constant, which depends on the initial value of streaming current and gate resistance.

From eqn (3) and (4), once  $\frac{nmC_{\text{ind}}}{C_L} - \frac{1}{RC_L} > 0$ , such as in Kelvin's water dropper ( $m = 1$ ,  $R_L = +\infty$ ), a positive feedback results in fast increases of induction current, and thus an absolute value of the target voltage is obtained as time passes until voltage breakdown between two targets occurs; while when  $\frac{nmC_{\text{ind}}}{C_L} - \frac{1}{RC_L} < 0$ , such as when considerably low resistance is used in the voltage divider, a negative feedback system results in a decrease of the induction current from the initial value determined by the streaming current. Generally stated, if we use ohmic resistance dividers such that the fraction  $m$  of the target voltage applied to the gate remains constant, the induction current, as seen from eqn (3) and (4), will undergo either positive feedback (leading to overcharging) or negative feedback (leading to non-charging). For our system, the critical transition resistance from a non-charging state to an overcharging state can be calculated as  $R_{L,\text{critical}} = 1/nC_{\text{ind}} = 20 \text{ G}\Omega$  (assuming  $nC_{\text{ind}} = 0.05 \text{ nA V}^{-1}$ ). Series voltage divider ratios are calculated and discussed in Fig. S2.† As shown in the above experimental results however, this resistance value led to undercharging, which is not surprising as slight variations in all parameters will exist. The choice for the use of non-ohmic reversely connected diodes is motivated by these phenomena.

## Further discussion and conclusion

The experimental efficiency of the self-excited device, although reaching an appreciable value of about 18%, is much smaller than the maximal efficiency of 48% previously found when using a 30  $\mu\text{m}$  pore and a voltage source for gating.<sup>1</sup> We expect that this is mainly due to the larger working distance between gate and target in the self-excited

system used here, which leads to energy loss due to air friction acting on the droplets. As we showed in the previous work, the system efficiency is a function of the distance between the target and the gate ring, and in the present device for ease of operation, we needed to create additional space to electrically connect the gate. In the future however, we expect that efficiency can be improved by redesigning the gating system. Another reason for the lower efficiency, as discussed above, is the formation of a droplet spray cone instead of a droplet train due to droplet repulsion when droplets become highly charged. As a result, the trajectory distances for droplets at the inside and outside of this cone are different, causing easier deflection for the droplets at the outside of the cone and decreasing the total energy conversion efficiency. It is therefore preferable to use a hemispherical target and place the pore at its center so that all the droplets have the same trajectory distance. In addition, a better target design without Delrin cover is preferable to fully collect the charged droplets.

The self-excited ballistic energy conversion system conceptually is similar to the Kelvin's water dropper, although the systems fundamentally differ in driving force (pressure or gravity) and energy conversion mechanism (inertial to electrical energy or gravitational to electrical). Interestingly, no theoretical analysis on the energy conversion efficiency of Kelvin's water dropper has been made yet. However, theoretically the energy loss is expected to be quite low due to the low surface energy (large droplets) and air friction (low droplet velocity). However, the real-life limitation of Kelvin's water dropper is the need for an extremely high voltage on the collector due to its large size and the small charge-to-mass ratio. In our case, micrometer-sized droplets are produced from the pore which can have a very high charge-to-mass ratio, so that the target voltage can be much lower (down to hundreds of volts as shown in the previous work). Besides, much less volume flow of water is needed in ballistic energy conversion than Kelvin's water dropper. Finally, it will be also possible to vary the operational current mode of the current device. A theoretical analysis and an equivalent circuit were designed to explain the unstable current induction in the resistance divider mode and stable current induction in the diode divider mode. A further refinement will be in DC or AC operation. Here we present a DC voltage microfluidic energy harvesting device. However, it has been shown that by proper design and connection of the circuit the Kelvin's droplet generator can also operate in AC mode, which will also be true for this ballistic version.<sup>14</sup>

Due to the high efficiency and power density of ballistic energy conversion systems, they can become a quite competitive method for renewable clean energy. For further application in daily life, this technology however needs to be developed by strongly integrating micropore membranes in complete closed systems, where, *e.g.*, the water transport is also managed. Systems with large pore arrays can be easily produced using clean room technology so that the power can be relatively easily increased. A first application area of such

devices would be in lab-on-a-chip systems that use high voltage, such as electrokinetic separation systems. When the operational voltage of the device can be further reduced by optimizing the gate potentials to less than 1 kV, other applications would also become feasible.

## Acknowledgements

Financial support through an NWO TOP grant (YX, AvdB, and JE) and the ERC grant ELab4Life (AvdB) is gratefully acknowledged.

## References

- 1 Y. Xie, D. Bos, L. J. de Vreede, H. L. de Boer, M.-J. van der Meulen, M. Versluis, A. J. Sprenkels, A. van den Berg and J. C. T. Eijkel, *Nat. Commun.*, 2014, 5, 3575.
- 2 R. B. M. Schasfoort, S. Schlautmann, L. Hendrikse and A. van den Berg, *Science*, 1999, 286, 942–945.
- 3 R. Karnik, K. Castelino, R. Fan, P. Yang and A. Majumdar, *Nano Lett.*, 2005, 5(9), 1638–1642.
- 4 A. I. Alolah, *Electr. Power Syst. Res.*, 1994, 31, 111–118.
- 5 J. Arrillaga and D. B. Watson, *Proc. Inst. Electr. Eng.*, 1978, 125, 743–746.
- 6 H. H. Sait, S. A. Daniel and P. M. Babu, *Tencon IEEE Region*, 2008, pp. 2391–2395.
- 7 G. K. Singh, *Electr. Power Syst. Res.*, 2004, 69, 107–114.
- 8 J. C. Wu, *IET Renewable Power Gener.*, 2009, 3, 144–151.
- 9 W. Thomson, *Proc. R. Soc. London*, 1867, 16, 67–72.
- 10 M. Ziaei-Moayyed, E. Goodman and P. Williams, *J. Chem. Educ.*, 2000, 77, 1520–1524.
- 11 Á. G. Marín, W. van Hoeve, P. García-Sánchez, L. Shui, Y. Xie, M. A. Fontelos, J. C. T. Eijkel, A. van den Berg and D. Lohse, *Lab Chip*, 2013, 13, 4503–4506.
- 12 J.-L. L. Abdil Ozdemir, K. J. Gillig and C.-H. Chen, *Analyst*, 2013, 138, 6913.
- 13 J. M. Schneide, N. R. Lindblad, C. D. Hendrick and J. M. Crowley, *J. Appl. Phys.*, 1967, 38, 2599–2605.
- 14 M. Zahn, *Am. J. Phys.*, 1973, 41, 196–202.